The Astrophysical Journal, 752:5 (13pp), 2012 June 10 doi:10.1088/0004-637X/752/1/5

THE $UBV(RI)_C$ COLORS OF THE SUN

I. Ramírez[1], R. Michel[2], R. Sefako[3], M. Tucci Maia[4,5], W. J. Schuster[2], F. van Wyk[3], J. Meléndez[5], L. Casagrande[6], and B. V. Castilho[7]

[1] McDonald Observatory and Department of Astronomy, University of Texas at Austin, 1 University Station, C1400 Austin, TX 78712-0259, USA
[2] Observatorio Astronómico Nacional, Universidad Nacional Autónoma de México, Apartado Postal 877, Ensenada, B.C., CP 22800, Mexico
[3] South African Astronomical Observatory, P.O. Box 9, Observatory 7935, Cape Town, South Africa
[4] UNIFEI, DFQ–Instituto de Ciências Exatas, Universidade Federal de Itajubá, Itajubá MG, Brazil
[5] Departamento de Astronomia do IAG/USP, Universidade de São Paulo, Rua do Mãtao 1226, São Paulo, 05508-900 SP, Brazil
[6] Max-Planck-Institut für Astrophysik, Karl-Schwarzschild-Str. 1, Postfach 1317, D-85741 Garching, Germany
[7] Laboratório Nacional de Astrofísica/MCT, Rua Estados Unidos 154, 37504-364 Itajubá, MG, Brazil

Received 2012 February 22; accepted 2012 April 3; published 2012 May 18

ABSTRACT

Photometric data in the $UBV(RI)_C$ system have been acquired for 80 solar analog stars for which we have previously derived highly precise atmospheric parameters $T_{\rm eff}$, $\log g$, and [Fe/H] using high-resolution, high signal-to-noise ratio spectra. UBV and $(RI)_C$ data for 46 and 76 of these stars, respectively, are published for the first time. Combining our data with those from the literature, colors in the $UBV(RI)_C$ system, with $\simeq$0.01 mag precision, are now available for 112 solar analogs. Multiple linear regression is used to derive the solar colors from these photometric data and the spectroscopically derived $T_{\rm eff}$, $\log g$, and [Fe/H] values. To minimize the impact of systematic errors in the model-dependent atmospheric parameters, we use only the data for the 10 stars that most closely resemble our Sun, i.e., the solar twins, and derive the following solar colors: $(B-V)_\odot = 0.653 \pm 0.005$, $(U-B)_\odot = 0.166 \pm 0.022$, $(V-R)_\odot = 0.352 \pm 0.007$, and $(V-I)_\odot = 0.702 \pm 0.010$. These colors are consistent, within the 1σ errors, with those derived using the entire sample of 112 solar analogs. We also derive the solar colors using the relation between spectral-line–depth ratios and observed stellar colors, i.e., with a completely model-independent approach, and without restricting the analysis to solar twins. We find $(B-V)_\odot = 0.653 \pm 0.003$, $(U-B)_\odot = 0.158 \pm 0.009$, $(V-R)_\odot = 0.356 \pm 0.003$, and $(V-I)_\odot = 0.701 \pm 0.003$, in excellent agreement with the model-dependent analysis.

Key words: stars: fundamental parameters – Sun: fundamental parameters – techniques: photometric

Online-only material: color figure

1. INTRODUCTION

Our Sun is the primary reference in stellar astrophysics. Its fundamental parameters are known with a precision and accuracy far greater than those of any other astronomical object known. Observationally, however, comparing the Sun with the distant stars is not an easy task. Unless dedicated to solar observation, or carefully adapted for that purpose, telescopes and their instruments are designed to collect as much light as possible from faint targets. Any attempt to observe the Sun with the same instrumental setup used to observe the distant stars will suffer from saturation. Fortunately, the Sun as a star can be studied indirectly, in particular using stars that have spectral features very similar to those observed in the solar spectrum, i.e., solar analog stars (e.g., Cayrel de Strobel 1996).

A wealth of useful information on the physical properties of stars can be inferred from their photometry. Narrowband systems such as Strömgren's $uvby$-β (Strömgren 1963) and systems designed for very large, all-sky surveys such as the *ugriz* system (e.g., Fukugita et al. 1996) are in many ways superior, or at least complementary, to the Johnson–Cousins $UBV(RI)_C$ system (Johnson & Morgan 1953; Cousins 1976). Nevertheless, for historical reasons, one could argue that the latter is still one of the most important systems (e.g., Bessell 2005). Much of our knowledge on stars is based on this type of observational data, and it is no surprise that whenever a new photometric system is introduced, transformation equations to the $UBV(RI)_C$ system must be determined.

Theoretical models can be used to translate photometric data into physical parameters and vice versa. These relationships, however, must be able to reproduce very well the solar values, given the high precision and accuracy with which the solar properties are known. The problem is that the solar colors cannot be measured directly, i.e., in an identical fashion to those of the distant stars, as explained before. Since they need to be derived indirectly, they are typically very uncertain and not very useful for the calibration of stellar models: thus the need for refinement in the derivation of the solar colors whenever possible.

The solar colors in the $UBV(RI)_C$ system, in particular $(B-V)_\odot$, have been a subject of debate for many decades. Values found in the literature, as derived by many different authors using a variety of techniques, range from about 0.62 to 0.69. Using the effective temperature ($T_{\rm eff}$) versus $(B-V)$ relation of Casagrande et al. (2010), and adopting [Fe/H] = 0, one finds that this range of $(B-V)$ color corresponds to a $T_{\rm eff}$ range of 216 K. Such large uncertainty in a fundamental zero-point calibration represents a severe limitation for reliably constraining stellar models.

A few direct measurements of the $(B-V)$ solar color have been made (e.g., Stebbins & Kron 1957; Tüg & Schmidt-Kaler 1982), but the range of $(B-V)_\odot$ values reported is essentially the same as that corresponding to the indirect measurements, suggesting that instrumental effects are very difficult to control (e.g., van den Bergh 1965). Indirectly, the solar colors can be measured using samples of stars with known physical properties and interpolating the correlation between these parameters and observed colors to the solar values (e.g., Chmielewski 1981; Ramírez & Meléndez 2005b; Holmberg et al. 2006; Casagrande et al. 2010). In some cases, other types of observations, for example, spectroscopic or spectrophotometric, of the Sun and

the distant stars are used, in addition to the stellar photometry, to interpolate to the solar values (e.g., Clements & Neff 1979; Straizys & Valiauga 1994; Gray 1992). The large range of $(B-V)_{\odot}$ values found in the literature (0.62–0.69), and the fact that the average error in the $(B-V)$ values typically measured with present-day instrumentation for the distant stars is only about 0.01 mag, suggests that systematic errors are still the dominant source of uncertainty for indirect determinations of $(B-V)_{\odot}$. For older reviews and a complete list of references on $(B-V)_{\odot}$, we refer the reader to Chmielewski (1981, his Table 2) and Gray (1992, his Figure 1).

In a more recent revival of the $(B-V)_{\odot}$ debate, Ramírez & Meléndez (2005a, 2005b) and Casagrande et al. (2006) have both used the so-called infrared flux method (IRFM; Blackwell et al. 1979) to derive the effective temperatures of large samples of nearby stars with accurate $\log g$ and [Fe/H] values, which were then used to calibrate [Fe/H]-dependent $T_{\rm eff}$–color relations. Using the latter, interpolation to the solar $T_{\rm eff} = 5777$ K and [Fe/H] $= 0$ allowed them to infer $(B-V)_{\odot}$, among other solar colors. Interestingly, even though both groups used the same technique to derive the star's $T_{\rm eff}$ values, their inferred solar colors differ by about 0.03 mag. While Ramírez & Meléndez (2005b) suggest a "blue" $(B-V)_{\odot} = 0.619$, Casagrande et al. (2006) find a more "red" $(B-V)_{\odot} = 0.651$. Although in principle nearly consistent within the 1σ uncertainties, which are about 0.02 mag for each, this discrepancy has been traced back to a difference in the zero point of the absolute flux calibration in the IRFM. Casagrande et al. (2010) have fine-tuned this absolute calibration and validated their IRFM $T_{\rm eff}$ scale using interferometrically measured stellar angular diameters and *Hubble Space Telescope* spectrophotometry. Their implementation of the IRFM gives us the most reliable $T_{\rm eff}$ scale available today from which they infer $(B-V)_{\odot} = 0.641 \pm 0.024$. The relatively large size of the error bar compared to the typical error in $(B-V)$ measurements ($\simeq$0.01 mag) is due to the fact that $T_{\rm eff}$–color relations of a sample of stars covering a wide range of stellar parameters were used, thus propagating small, but non-negligible, systematic errors into the analysis.

In recent years, we have undertaken the task of studying solar twin and analog stars, i.e., stars with atmospheric parameters $T_{\rm eff}$, $\log g$, and [Fe/H] identical and very similar to those of our Sun, respectively. We have carried out spectroscopic surveys in both the southern and northern hemispheres, searching for these stars and performing unprecedentedly high precision spectroscopic analysis (e.g., Meléndez et al. 2006, 2009; Meléndez & Ramírez 2007; Ramírez et al. 2009). Surprisingly for us, before the present work, photometric data in the $UBV(RI)_{\rm C}$ system for the solar twins and analogs that we identified were scarce in the literature. For example, only about half of the stars of interest were found in the *UBV* section of the General Catalogue of Photometric Data (GCPD; Mermilliod et al. 1997) and the *Hipparcos* catalog $(B-V)$ compilation (Perryman et al. 1997). Motivated by this lack of fundamental, very important astronomical data, we have carried out campaigns to measure colors of solar analog stars in the $UBV(RI)_{\rm C}$ system at three different locations, which allowed us to cover the entire sky. In this paper, we present the photometric data acquired and use them along with our spectroscopically determined stellar atmospheric parameters, as well as the high-quality spectra themselves, to derive the solar $UBV(RI)_{\rm C}$ colors. We expect these solar colors to be both very precise and accurate because the sample selection guarantees that the impact of systematic errors is small. For the first time, a statistically significant sample of solar twins and analogs with highly precise differential stellar parameters derived from high-quality spectra, and homogeneously measured photometry, is available to derive the $UBV(RI)_{\rm C}$ colors of the Sun.

2. SAMPLE AND PHOTOMETRIC DATA

The stars used in this work are listed in Table 4 of Baumann et al. (2010), who studied the evolution of lithium abundances in Sun-like stars using high-resolution, high signal-to-noise ratio spectra acquired by Ramírez et al. (2009) and Meléndez et al. (2009). These spectra were taken using the R. G. Tull coudé spectrograph on the 2.7 m telescope at McDonald Observatory and the MIKE spectrograph on the 6.5 m Clay/Magellan Telescope at Las Campanas Observatory. The spectral resolution $R = \lambda/\Delta\lambda$ of the spectroscopic data is about 60,000 while the signal-to-noise ratios range from about 150 to 600, with a median value closer to 400. The stellar parameters $T_{\rm eff}$, $\log g$, and [Fe/H] used in this work are those listed in Baumann et al. (2010) and they were determined by forcing excitation/ionization equilibrium of iron lines in the stellar spectra. Given the high quality of the data and the careful sample selection, the average errors in the stellar parameters are only $\Delta T_{\rm eff} = 41$ K, $\Delta \log g = 0.06$, and Δ[Fe/H] $= 0.03$, although they are significantly smaller for the stars that are most similar to the Sun. Systematic errors are not included in these error estimates, but we expect them to be very small because of the strictly differential approach we used to derive the atmospheric parameters. All of the objects analyzed in the present study are main-sequence stars, as confirmed by their $\log g$ values. We refer the reader to Meléndez et al. (2009), Ramírez et al. (2009), and Baumann et al. (2010) for details on the spectroscopic data reduction, the determination of stellar parameters, and the assessment of errors.

$UBV(RI)_{\rm C}$ magnitudes and colors for as many as possible of the stars in Baumann et al. (2010) were measured at three sites: SAAO (South African Astronomical Observatory), SPM (San Pedro Martir, in Mexico), and OPD (Observatório do Pico dos Dias, in Brazil); 57 stars were observed at SAAO, 55 at SPM, and 33 at OPD. A number of stars were observed at more than one location; the total number of unique stars observed is 80. Below we describe briefly our photometric observations.

The SAAO $UBV(RI)_{\rm C}$ observations were made using the 0.5 m telescope and a photomultiplier tube (PMT) based modular photometer at Sutherland (Kilkenny et al. 1988). The PMT is a Hamamatsu R943-02 Gallium Arsenide tube and it is thermoelectrically cooled to low temperatures to reduce dark counts to minimum levels. Observations were carried out throughout 2010 and 2011 in blocks of several weeks spread over the two years. Observations of both the target objects and E-region standard stars (e.g., Menzies et al. 1989) were made each night through the $UBV(RI)_{\rm C}$ filters, mostly alternating between a standard and a target object. The observations were later corrected to the $UBV(RI)_{\rm C}$ system using nightly observations of the E-region standards and current transformation equations that are maintained and regularly updated (about twice a year) at the Observatory. Observations were done only during photometric nights, and any standard star observations that deviate from the standard magnitude by more than $\pm$0.05 are not used in the reduction or determination of zero points for transformation to the $UBV(RI)_{\rm C}$ system. Based on the observations of standard stars made in multiple observing nights and/or runs, we estimate an accuracy of about 0.01 mag for the SAAO measurements of

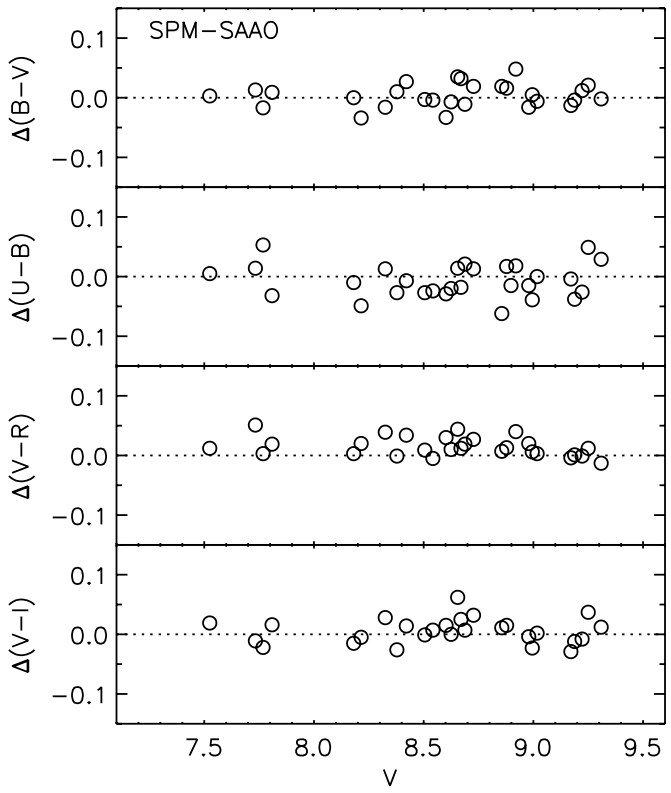

Figure 1. Difference in color measured at the SPM and SAAO observatories as a function of apparent visual magnitude, as observed from SAAO.

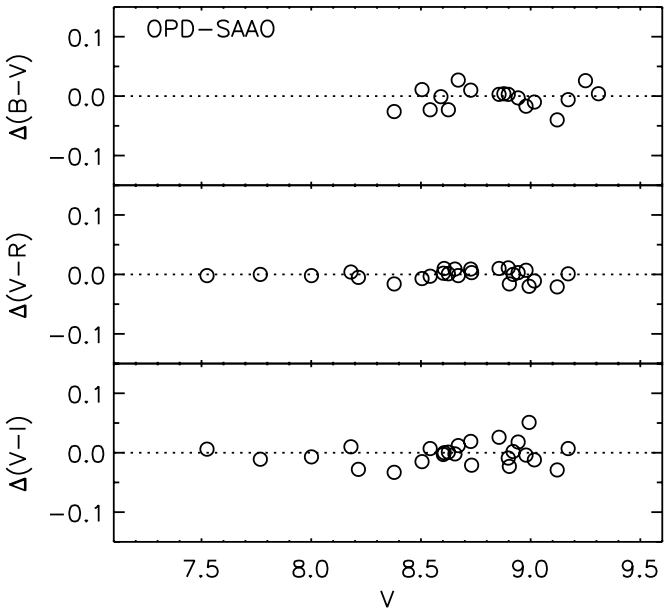

Figure 2. Difference in color measured at the OPD and SAAO observatories as a function of apparent visual magnitude, as observed from SAAO.

visual magnitudes and colors. The E-region stars used in our reductions have visual magnitudes from about $V = 5$ to $V = 10$, which is similar to the magnitude range of our observed program stars.

The SPM observations were carried out during two runs; eight nights in 2011 May (from the 21st to the 28th) and five nights in 2011 October (from the 20th to the 24th). The San Pedro Martir 0.84 m telescope was used, along with the Mexman filter wheel. During the May run a SITe CCD was used (1024 × 1024 pixels, gain = 4.8 e^- ADU^{-1}, readout noise = 13 e^-) while in October an e2v-4290 CCD was used (4.5 K × 2 K pixels, gain = 1.7 e^- ADU^{-1}, readout noise = 3.8 e^-). Sky flat fields were taken at the beginning and end of each night, and bias frames were taken between each observed field. Landolt standards were observed both at the meridian and at large air masses. All the images were bias subtracted and flat field corrected. Cosmic rays were removed using the L.A. Cosmic task (van Dokkum 2001). Instrumental magnitudes were calculated using the IRAF "photcal" package and the observations of the standard stars.

The OPD photometric data were acquired using the Zeiss 0.6 m telescope at Pico dos Dias Observatory, operated by the Laboratório Nacional de Astrofísica, in Brazil, during the years 2009 and 2010. The instrument used for the observation was the FOTRAP ("rapid photometer"; Jablonski et al. 1994), which consists of a wheel with six filters (Johnson–Cousins $UBV(RI)_C$ and clear) running at 20 Hz and acquiring data almost simultaneously in all filters. Light from the telescope passes through the filter wheel and then by a set of diaphragms that is used for limiting interference of light from the sky and/or nearby objects. Then the light reaches the Hamamatsu photomultiplier operating at −25°C. Throughout the night, various Graham (1982) standard stars are observed. Usually, one in every three stars observed was a standard, making sure no star with an airmass greater than 1.5 was observed, following the suggestion by Harris et al. (1981), whose photometric reduction method is used in the reduction software of this instrument. The reduction is made using the software "mags.exe," which was specially written for the instrument FOTRAP, as described in Jablonski et al. (1994).

The photometric data collected at the three sites described above are given in Tables 1–3. Figure 1 shows the comparison of colors measured at the SPM and SAAO observatories for the stars in common. Similarly, Figure 2 shows the comparison of OPD and SAAO data. In Table 4 we list the mean offsets and the star-to-star standard deviation of the difference between colors measured at different sites, determined using data for stars in common between the different samples. In most cases the mean differences are compatible with zero within the 1σ uncertainties, suggesting that any offsets that could be a product of employing different sets of photometric standard stars and/or data reduction procedures are smaller than the observational errors. The only exception is the SPM $(V - R)$ data set, which shows a non-zero mean offset of 0.021 ± 0.016 relative to the SAAO data. To prevent this offset from introducing unwanted noise in our solar colors analysis, we corrected the SPM $(V - R)$ colors so that their mean difference with the SAAO data is exactly zero. The values listed in Table 2, however, are the original ones.

For the stars that were observed from more than one location, we adopted a weighted mean of the colors given from each site. The error associated with these average colors corresponds to the sample variance. However, we adopted a minimum photometric error of 0.004 mag to prevent unreasonably small errors arising from numerical artifacts, i.e., from coincidental agreement between the (statistically few) mean values reported from different sites.

We also searched for $UBV(RI)_C$ photometry in the GCPD (Mermilliod et al. 1997) and $(B - V)$ colors in the *Hipparcos* catalog (Perryman et al. 1997) for the stars in Baumann et al. (2010). We used the latter only if not available in the GCDP. These *Hipparcos* $(B - V)$ colors correspond to those compiled by the mission team from previously published

Table 1
SAAO Photometry

HIP	V	$(B-V)$	$(U-B)$	$(V-R)$	$(V-I)$	N_{obs}
348	8.602 ± 0.015	0.669 ± 0.015	0.124 ± 0.015	0.346 ± 0.015	0.691 ± 0.015	1
996	8.215 ± 0.015	0.664 ± 0.015	0.163 ± 0.015	0.352 ± 0.015	0.694 ± 0.015	1
1499	6.474 ± 0.012	0.687 ± 0.008	0.257 ± 0.008	0.368 ± 0.005	0.715 ± 0.005	2
4909	8.505 ± 0.025	0.636 ± 0.006	0.133 ± 0.015	0.363 ± 0.013	0.689 ± 0.016	2
5134	8.979 ± 0.009	0.640 ± 0.004	0.081 ± 0.015	0.345 ± 0.008	0.706 ± 0.013	2
6407	8.625 ± 0.004	0.656 ± 0.004	0.144 ± 0.015	0.360 ± 0.011	0.704 ± 0.015	2
8507	8.898 ± 0.004	0.651 ± 0.006	0.141 ± 0.023	0.359 ± 0.011	0.730 ± 0.007	2
8841	9.246 ± 0.006	0.669 ± 0.004	0.157 ± 0.014	0.378 ± 0.004	0.729 ± 0.015	2
9349	7.991 ± 0.004	0.650 ± 0.004	0.147 ± 0.008	0.343 ± 0.004	0.691 ± 0.012	2
11915	8.615 ± 0.008	0.653 ± 0.004	0.134 ± 0.004	0.354 ± 0.004	0.699 ± 0.004	2
28336	8.995 ± 0.015	0.642 ± 0.015	0.130 ± 0.015	0.360 ± 0.015	0.710 ± 0.015	1
30037	9.162 ± 0.015	0.682 ± 0.015	0.213 ± 0.015	0.361 ± 0.015	0.706 ± 0.015	1
30502	8.667 ± 0.015	0.664 ± 0.015	0.152 ± 0.015	0.368 ± 0.015	0.707 ± 0.015	1
36512	7.733 ± 0.004	0.655 ± 0.005	0.120 ± 0.004	0.355 ± 0.005	0.696 ± 0.015	2
38072	9.222 ± 0.004	0.648 ± 0.004	0.151 ± 0.011	0.363 ± 0.006	0.701 ± 0.004	2
39748	8.591 ± 0.006	0.615 ± 0.011	0.050 ± 0.004	0.340 ± 0.008	0.681 ± 0.004	2
41317	7.809 ± 0.006	0.664 ± 0.008	0.159 ± 0.004	0.367 ± 0.004	0.714 ± 0.011	2
43190	8.508 ± 0.015	0.670 ± 0.015	0.232 ± 0.015	0.370 ± 0.015	0.696 ± 0.015	1
44935	8.688 ± 0.015	0.654 ± 0.015	0.182 ± 0.015	0.345 ± 0.015	0.684 ± 0.015	1
44997	8.325 ± 0.015	0.666 ± 0.015	0.191 ± 0.015	0.344 ± 0.015	0.685 ± 0.015	1
46126	8.514 ± 0.006	0.653 ± 0.010	0.167 ± 0.006	0.354 ± 0.006	0.704 ± 0.023	2
49756	7.525 ± 0.015	0.644 ± 0.015	0.181 ± 0.015	0.349 ± 0.015	0.672 ± 0.015	1
51258	7.874 ± 0.004	0.730 ± 0.004	0.344 ± 0.008	0.386 ± 0.006	0.735 ± 0.004	2
54102	8.653 ± 0.004	0.649 ± 0.004	0.142 ± 0.015	0.346 ± 0.004	0.698 ± 0.004	2
55409	8.001 ± 0.010	0.657 ± 0.011	0.174 ± 0.017	0.368 ± 0.007	0.720 ± 0.008	2
57291	7.466 ± 0.008	0.740 ± 0.004	0.354 ± 0.006	0.375 ± 0.016	0.732 ± 0.013	2
59357	8.655 ± 0.008	0.627 ± 0.008	0.076 ± 0.004	0.344 ± 0.004	0.684 ± 0.007	2
60081	8.023 ± 0.007	0.696 ± 0.006	0.290 ± 0.008	0.373 ± 0.007	0.702 ± 0.007	2
60370	6.703 ± 0.004	0.651 ± 0.004	0.148 ± 0.013	0.349 ± 0.008	0.674 ± 0.008	2
60653	8.731 ± 0.015	0.638 ± 0.015	0.109 ± 0.015	0.358 ± 0.015	0.715 ± 0.015	1
64150	6.761 ± 0.007	0.688 ± 0.016	0.200 ± 0.004	0.349 ± 0.017	0.694 ± 0.004	2
64497	8.920 ± 0.004	0.653 ± 0.004	0.176 ± 0.004	0.357 ± 0.004	0.686 ± 0.013	2
64713	9.250 ± 0.004	0.648 ± 0.004	0.138 ± 0.004	0.355 ± 0.010	0.690 ± 0.010	2
64794	8.421 ± 0.006	0.640 ± 0.006	0.150 ± 0.016	0.343 ± 0.010	0.696 ± 0.016	2
64993	8.878 ± 0.004	0.650 ± 0.007	0.155 ± 0.013	0.352 ± 0.006	0.697 ± 0.007	2
66885	9.309 ± 0.005	0.630 ± 0.012	0.067 ± 0.018	0.366 ± 0.004	0.729 ± 0.004	2
69063	8.882 ± 0.006	0.632 ± 0.004	0.068 ± 0.004	0.352 ± 0.004	0.706 ± 0.010	2
73815	8.181 ± 0.011	0.668 ± 0.008	0.171 ± 0.011	0.360 ± 0.006	0.698 ± 0.004	2
74389	7.768 ± 0.010	0.640 ± 0.014	0.149 ± 0.007	0.349 ± 0.004	0.689 ± 0.004	2
75923	9.171 ± 0.014	0.664 ± 0.006	0.138 ± 0.004	0.367 ± 0.018	0.718 ± 0.007	2
77883	8.727 ± 0.006	0.681 ± 0.004	0.214 ± 0.011	0.368 ± 0.004	0.719 ± 0.004	2
79304	8.670 ± 0.006	0.629 ± 0.007	0.166 ± 0.006	0.353 ± 0.011	0.680 ± 0.004	2
79578	6.533 ± 0.033	0.678 ± 0.028	0.145 ± 0.012	0.352 ± 0.008	0.699 ± 0.004	2
79672	5.503 ± 0.015	0.644 ± 0.015	0.157 ± 0.015	0.354 ± 0.015	0.704 ± 0.015	1
82853	8.993 ± 0.026	0.660 ± 0.020	0.181 ± 0.004	0.396 ± 0.004	0.728 ± 0.006	2
83707	8.606 ± 0.015	0.655 ± 0.004	0.181 ± 0.004	0.348 ± 0.011	0.699 ± 0.007	2
85042	6.287 ± 0.004	0.669 ± 0.004	0.207 ± 0.017	0.364 ± 0.020	0.707 ± 0.051	2
85272	9.121 ± 0.010	0.640 ± 0.011	0.095 ± 0.012	0.368 ± 0.011	0.718 ± 0.008	2
85285	8.378 ± 0.019	0.632 ± 0.008	0.076 ± 0.018	0.363 ± 0.019	0.715 ± 0.005	2
86796	5.124 ± 0.006	0.681 ± 0.028	0.296 ± 0.017	0.386 ± 0.005	0.706 ± 0.005	2
89162	8.903 ± 0.007	0.658 ± 0.005	0.176 ± 0.004	0.363 ± 0.010	0.698 ± 0.011	2
89650	8.943 ± 0.010	0.644 ± 0.006	0.126 ± 0.004	0.354 ± 0.010	0.679 ± 0.013	2
91332	7.971 ± 0.008	0.696 ± 0.009	0.263 ± 0.004	0.365 ± 0.015	0.705 ± 0.004	2
102152	9.188 ± 0.013	0.671 ± 0.018	0.196 ± 0.023	0.382 ± 0.004	0.727 ± 0.004	2
104504	8.542 ± 0.015	0.640 ± 0.015	0.081 ± 0.015	0.366 ± 0.015	0.696 ± 0.015	1
108996	8.856 ± 0.015	0.640 ± 0.015	0.165 ± 0.015	0.350 ± 0.015	0.677 ± 0.015	1
118159	9.017 ± 0.004	0.633 ± 0.018	0.090 ± 0.015	0.355 ± 0.014	0.679 ± 0.005	2

standard *UBV* system data sets (i.e., those with flag G in Column 39 of the *Hipparcos* catalog) and not to the colors inferred from transformation equations using *Tycho* photometry (flag T instead). Sixty-six stars were found with either *UBV* and/or $RI_{(C)}$ colors previously reported in the literature. Thirty-four of these stars were observed by us. However, only four of them have $RI_{(C)}$ data in the literature. Thus, a proper comparison of our measured colors with previously published values can only be done for $(B-V)$ and $(U-B)$. This comparison is shown in Figure 3.

The average difference in $(B-V)$ color between our measurements and those found in the literature is

Table 2
SPM Photometry

HIP	V	$(B-V)$	$(U-B)$	$(V-R)$	$(V-I)$	N_{obs}
348	8.595 ± 0.020	0.636 ± 0.022	0.095 ± 0.021	0.376 ± 0.036	0.706 ± 0.022	1
996	8.189 ± 0.009	0.630 ± 0.012	0.114 ± 0.021	0.372 ± 0.011	0.689 ± 0.011	1
2131	8.923 ± 0.008	0.642 ± 0.011	0.106 ± 0.023	0.376 ± 0.009	0.720 ± 0.009	1
2894	8.651 ± 0.018	0.659 ± 0.028	0.200 ± 0.039	0.371 ± 0.034	0.703 ± 0.019	1
4909	8.515 ± 0.009	0.633 ± 0.011	0.106 ± 0.014	0.372 ± 0.012	0.688 ± 0.013	1
5134	8.969 ± 0.007	0.624 ± 0.009	0.066 ± 0.017	0.365 ± 0.010	0.702 ± 0.008	1
6407	8.613 ± 0.021	0.649 ± 0.022	0.124 ± 0.017	0.370 ± 0.035	0.704 ± 0.021	1
7245	8.361 ± 0.009	0.667 ± 0.013	0.186 ± 0.022	0.376 ± 0.011	0.691 ± 0.011	1
8507	...	...	0.126 ± 0.014	...	...	1
9349	8.220 ± 0.054	...	...	...	...	1
18261	7.980 ± 0.027	0.616 ± 0.029	0.083 ± 0.017	0.348 ± 0.047	0.670 ± 0.028	1
25670	8.275 ± 0.021	0.663 ± 0.023	0.167 ± 0.012	0.362 ± 0.036	0.698 ± 0.024	1
28336	8.998 ± 0.005	0.647 ± 0.013	0.091 ± 0.013	0.366 ± 0.017	0.687 ± 0.026	1
36512	7.700 ± 0.011	0.668 ± 0.019	0.134 ± 0.019	0.406 ± 0.029	0.685 ± 0.099	1
38072	9.214 ± 0.016	0.660 ± 0.025	0.125 ± 0.027	0.362 ± 0.026	0.693 ± 0.021	2
41317	7.798 ± 0.015	0.673 ± 0.023	0.127 ± 0.029	0.386 ± 0.034	0.730 ± 0.024	1
44324	7.943 ± 0.010	0.620 ± 0.027	0.083 ± 0.035	0.342 ± 0.011	0.674 ± 0.016	4
44935	8.743 ± 0.004	0.643 ± 0.006	0.203 ± 0.006	0.364 ± 0.006	0.691 ± 0.006	1
44997	8.370 ± 0.015	0.650 ± 0.016	0.204 ± 0.007	0.383 ± 0.027	0.713 ± 0.016	1
46066	8.928 ± 0.007	0.664 ± 0.017	0.188 ± 0.016	0.381 ± 0.008	0.717 ± 0.008	2
49572	9.288 ± 0.006	0.640 ± 0.007	0.138 ± 0.006	0.357 ± 0.008	0.702 ± 0.007	1
49756	7.540 ± 0.004	0.647 ± 0.006	0.186 ± 0.006	0.361 ± 0.006	0.691 ± 0.006	1
55459	7.646 ± 0.004	0.646 ± 0.006	0.153 ± 0.006	0.359 ± 0.006	0.692 ± 0.006	1
56948	8.669 ± 0.004	0.646 ± 0.006	0.180 ± 0.006	0.360 ± 0.006	0.680 ± 0.006	1
59357	8.752 ± 0.004	0.662 ± 0.010	0.090 ± 0.011	0.388 ± 0.006	0.746 ± 0.006	1
60314	8.780 ± 0.008	0.665 ± 0.009	0.155 ± 0.007	0.358 ± 0.011	0.676 ± 0.009	1
62175	8.011 ± 0.005	0.656 ± 0.006	0.194 ± 0.007	0.366 ± 0.006	0.682 ± 0.006	1
64150	6.883 ± 0.007	0.717 ± 0.008	0.217 ± 0.006	0.402 ± 0.009	0.724 ± 0.008	1
64497	9.035 ± 0.004	0.701 ± 0.006	0.194 ± 0.006	0.397 ± 0.006	...	1
64713	9.297 ± 0.008	0.669 ± 0.020	0.187 ± 0.019	0.367 ± 0.012	0.727 ± 0.009	1
64794	8.461 ± 0.020	0.667 ± 0.020	0.143 ± 0.006	0.377 ± 0.030	0.710 ± 0.020	1
64993	8.921 ± 0.004	0.666 ± 0.009	0.172 ± 0.009	0.365 ± 0.006	0.712 ± 0.006	1
66885	9.274 ± 0.010	0.628 ± 0.023	0.096 ± 0.024	0.353 ± 0.016	0.741 ± 0.011	1
73815	8.173 ± 0.005	0.668 ± 0.006	0.161 ± 0.008	0.363 ± 0.006	0.683 ± 0.009	2
74341	8.857 ± 0.005	0.673 ± 0.014	0.165 ± 0.018	0.354 ± 0.016	0.684 ± 0.009	3
74389	7.760 ± 0.021	0.623 ± 0.024	0.202 ± 0.024	0.352 ± 0.022	0.667 ± 0.023	1
75923	9.149 ± 0.005	0.651 ± 0.006	0.134 ± 0.006	0.363 ± 0.007	0.689 ± 0.006	1
77883	8.770 ± 0.004	0.700 ± 0.006	0.227 ± 0.006	0.395 ± 0.006	0.751 ± 0.006	1
78028	8.651 ± 0.012	0.638 ± 0.019	0.118 ± 0.024	0.355 ± 0.016	0.683 ± 0.016	5
78680	8.243 ± 0.013	0.626 ± 0.018	0.079 ± 0.021	0.358 ± 0.016	0.698 ± 0.016	3
79186	8.341 ± 0.014	0.675 ± 0.028	0.140 ± 0.033	0.377 ± 0.022	0.724 ± 0.018	3
79304	8.718 ± 0.004	0.661 ± 0.007	0.148 ± 0.008	0.365 ± 0.006	0.705 ± 0.011	2
79672	5.522 ± 0.019	0.680 ± 0.019	0.182 ± 0.006	0.401 ± 0.019	0.773 ± 0.019	2
81512	9.245 ± 0.015	0.652 ± 0.017	0.140 ± 0.019	0.374 ± 0.019	0.712 ± 0.016	3
85285	8.356 ± 0.010	0.642 ± 0.020	0.049 ± 0.021	0.362 ± 0.013	0.689 ± 0.017	3
88194	7.084 ± 0.011	0.656 ± 0.012	0.132 ± 0.016	0.390 ± 0.016	0.723 ± 0.018	3
88427	9.329 ± 0.006	0.638 ± 0.013	0.089 ± 0.022	0.357 ± 0.018	0.704 ± 0.007	1
89443	8.843 ± 0.004	0.660 ± 0.007	0.147 ± 0.013	0.380 ± 0.006	0.715 ± 0.006	1
100963	7.081 ± 0.009	0.651 ± 0.014	0.128 ± 0.024	0.359 ± 0.010	0.708 ± 0.010	1
102152	9.220 ± 0.010	0.667 ± 0.017	0.158 ± 0.022	0.383 ± 0.032	0.715 ± 0.016	1
104504	8.594 ± 0.020	0.636 ± 0.022	0.057 ± 0.014	0.361 ± 0.039	0.703 ± 0.021	1
108708	8.945 ± 0.017	0.659 ± 0.020	0.162 ± 0.012	0.379 ± 0.036	0.707 ± 0.021	1
108996	8.889 ± 0.009	0.659 ± 0.010	0.103 ± 0.029	0.357 ± 0.010	0.688 ± 0.014	2
109931	8.956 ± 0.019	0.674 ± 0.020	0.204 ± 0.020	0.388 ± 0.034	0.710 ± 0.020	1
118159	9.004 ± 0.004	0.627 ± 0.007	0.090 ± 0.014	0.358 ± 0.007	0.681 ± 0.006	1

$\Delta(B-V) = 0.002 \pm 0.011$, i.e., consistent with zero within the 1σ uncertainty. Moreover, the star-to-star scatter in this comparison (0.011 mag) suggests that the mean error in the measurements of $(B-V)$ is about 0.008 mag $= 0.011/\sqrt{2}$, which is identical to the average $(B-V)$ error given in our Table 5. Thus, our $(B-V)$ error estimates appear to be very reliable. For $(U-B)$, we derive $\Delta(U-B) = 0.013 \pm 0.034$, also consistent with zero within the uncertainties. We also computed offsets for $(V-R)$ and $(V-I)$, but they are based on data for only four stars in common and are therefore not so reliable. In any case, this comparison suggests that our color measurements are consistent with the $UBV(RI)_C$ color scales found in the literature and

Table 3
OPD Photometry

HIP	V	$(B-V)$	$(V-R)$	$(V-I)$	N_{obs}
348	8.604 ± 0.026	...	0.348 ± 0.017	0.688 ± 0.035	1
996	8.216 ± 0.028	...	0.347 ± 0.018	0.666 ± 0.037	1
4909	8.498 ± 0.024	0.647 ± 0.015	0.356 ± 0.016	0.674 ± 0.032	1
5134	8.970 ± 0.025	0.623 ± 0.016	0.352 ± 0.016	0.702 ± 0.034	1
6407	8.617 ± 0.025	0.633 ± 0.016	0.361 ± 0.016	0.705 ± 0.034	1
7245	8.366 ± 0.032	...	0.350 ± 0.021	0.685 ± 0.043	1
8507	8.924 ± 0.024	0.654 ± 0.016	0.370 ± 0.016	0.721 ± 0.033	1
39748	8.675 ± 0.058	0.614 ± 0.067	...	...	2
49756	7.577 ± 0.020	...	0.347 ± 0.010	0.678 ± 0.012	2
55409	8.149 ± 0.102	...	0.366 ± 0.020	0.713 ± 0.025	3
59357	8.676 ± 0.020	...	0.353 ± 0.009	0.682 ± 0.012	3
60653	8.742 ± 0.020	...	0.361 ± 0.009	0.694 ± 0.012	3
64497	8.995 ± 0.020	...	0.357 ± 0.009	0.688 ± 0.012	3
64713	9.429 ± 0.057	0.674 ± 0.065	...	...	2
64794	8.867 ± 0.064	...	...	...	3
73815	8.137 ± 0.108	...	0.364 ± 0.021	0.708 ± 0.026	1
74341	8.917 ± 0.022	...	0.355 ± 0.011	0.699 ± 0.013	3
74389	7.803 ± 0.020	...	0.349 ± 0.009	0.678 ± 0.012	3
75923	9.182 ± 0.012	0.658 ± 0.011	0.368 ± 0.009	0.725 ± 0.014	3
77883	8.734 ± 0.011	0.691 ± 0.011	0.377 ± 0.009	0.738 ± 0.013	3
79304	8.703 ± 0.013	0.656 ± 0.014	0.351 ± 0.011	0.692 ± 0.016	3
82853	8.018 ± 0.151	...	0.376 ± 0.031	0.779 ± 0.038	1
83707	8.528 ± 0.108	...	0.358 ± 0.021	0.699 ± 0.026	1
85272	9.120 ± 0.030	0.600 ± 0.022	0.347 ± 0.019	0.689 ± 0.039	1
85285	8.400 ± 0.025	0.606 ± 0.017	0.347 ± 0.017	0.682 ± 0.034	2
88194	7.171 ± 0.022	...	0.356 ± 0.011	0.706 ± 0.014	2
89162	8.882 ± 0.031	...	0.347 ± 0.020	0.675 ± 0.041	2
89650	8.946 ± 0.011	0.641 ± 0.010	0.357 ± 0.009	0.697 ± 0.013	5
100963	7.140 ± 0.022	...	0.346 ± 0.011	0.694 ± 0.014	2
104504	8.532 ± 0.010	0.617 ± 0.008	0.363 ± 0.008	0.703 ± 0.012	3
108708	8.937 ± 0.010	0.659 ± 0.008	0.368 ± 0.008	0.712 ± 0.012	3
108996	8.881 ± 0.010	0.643 ± 0.008	0.360 ± 0.008	0.703 ± 0.012	3
118159	9.005 ± 0.025	0.623 ± 0.016	0.344 ± 0.016	0.667 ± 0.033	1

Table 4
Photometry Offsets

Δ(color)	Mean	σ	n[a]
SPM–SAAO			
$\Delta(B-V)$	0.011	0.022	28
$\Delta(U-B)$	0.001	0.021	29
$\Delta(V-R)$	0.021	0.016	28
$\Delta(V-I)$	0.011	0.024	27
OPD–SAAO			
$\Delta(B-V)$	−0.004	0.016	17
$\Delta(V-R)$	0.001	0.007	25
$\Delta(V-I)$	0.002	0.015	25
TW–LIT			
$\Delta(B-V)$	0.002	0.011	34
$\Delta(U-B)$	0.013	0.034	14
$\Delta(V-R)$	0.007	0.006	4
$\Delta(V-I)$	0.006	0.013	4

Note. [a] n is the number of stars in common between the two samples.

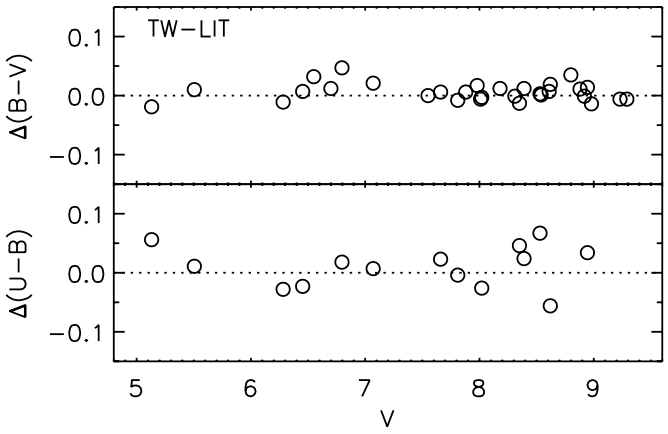

Figure 3. Difference in color measured by us and those found in the literature as a function of apparent visual magnitude, as found in the literature.

therefore with the historically adopted photometric zero points. The color offsets between our data (TW) and previously published values (LIT) are given in the lower section of Table 4.

The stellar parameters and photometry adopted in this work are given in Table 5. Here we have combined our photometric data with those found in the literature, giving equal weight to each when available for the same star. Objects for which photometric data are published for the first time are assigned mean values and errors from our measurements only. Stars not observed photometrically by us, but found in the literature, are assigned those previously published values. The average errors, in mag, of the measured colors given in Table 5 are $\Delta(B-V) = 0.008$, $\Delta(U-B) = 0.012$, $\Delta(V-R) = 0.010$, and $\Delta(V-I) = 0.010$.

Table 5
Adopted Stellar Parameters and Photometry

HIP	$T_{\rm eff}$ (K)	$\log g$	[Fe/H]	V	$(B-V)$	$(U-B)$	$(V-R)$	$(V-I)$	$N_{\rm obs}$[a]	Source[b]
348	5777 ± 40	4.41 ± 0.07	−0.130 ± 0.024	8.600 ± 0.004	0.644 ± 0.008	0.151 ± 0.026	0.348 ± 0.004	0.695 ± 0.007	3	SPM+SAAO+OPD+LIT
996	5860 ± 41	4.38 ± 0.07	0.000 ± 0.022	8.197 ± 0.012	0.643 ± 0.019	0.146 ± 0.023	0.351 ± 0.004	0.689 ± 0.006	3	SPM+SAAO+OPD
1499	5756 ± 44	4.37 ± 0.05	0.189 ± 0.015	6.474 ± 0.012	0.680 ± 0.004	0.265 ± 0.011	0.368 ± 0.004	0.714 ± 0.004	2	SAAO+LIT
2131	5720 ± 41	4.38 ± 0.07	−0.210 ± 0.026	8.923 ± 0.008	0.643 ± 0.004	0.106 ± 0.023	0.355 ± 0.009	0.720 ± 0.009	1	SPM+LIT
2894	5820 ± 44	4.54 ± 0.07	−0.030 ± 0.025	8.651 ± 0.018	0.659 ± 0.028	0.200 ± 0.039	0.350 ± 0.034	0.703 ± 0.019	1	SPM
4909	5836 ± 54	4.44 ± 0.07	0.020 ± 0.024	8.512 ± 0.006	0.637 ± 0.004	0.119 ± 0.013	0.357 ± 0.005	0.687 ± 0.004	4	SPM+SAAO+OPD
5134	5779 ± 38	4.49 ± 0.07	−0.190 ± 0.023	8.973 ± 0.005	0.637 ± 0.007	0.074 ± 0.007	0.346 ± 0.004	0.703 ± 0.004	4	SPM+SAAO+OPD
6407	5787 ± 25	4.47 ± 0.03	−0.090 ± 0.011	8.624 ± 0.002	0.652 ± 0.005	0.135 ± 0.010	0.360 ± 0.004	0.704 ± 0.004	4	SPM+SAAO+OPD+LIT
7245	5843 ± 47	4.53 ± 0.07	0.100 ± 0.023	8.361 ± 0.001	0.675 ± 0.006	0.148 ± 0.017	0.354 ± 0.004	0.691 ± 0.004	2	SPM+OPD+LIT
8507	5720 ± 55	4.44 ± 0.08	−0.080 ± 0.026	8.899 ± 0.004	0.651 ± 0.004	0.130 ± 0.007	0.363 ± 0.005	0.730 ± 0.004	4	SPM+SAAO+OPD
8841	5676 ± 45	4.50 ± 0.06	−0.120 ± 0.021	9.246 ± 0.006	0.674 ± 0.004	0.157 ± 0.014	0.378 ± 0.004	0.729 ± 0.015	2	SAAO+LIT
9349	5825 ± 28	4.49 ± 0.06	0.010 ± 0.017	7.992 ± 0.017	0.650 ± 0.004	0.147 ± 0.008	0.343 ± 0.004	0.691 ± 0.004	3	SPM+SAAO
11072	5897 ± 84	4.01 ± 0.06	−0.037 ± 0.057	5.190 ± 0.007	0.597 ± 0.004	0.120 ± 0.004	0.355 ± 0.020	0.692 ± 0.020	0	LIT
11728	5738 ± 30	4.37 ± 0.05	0.045 ± 0.019	...	0.666 ± 0.015	...	...	...	0	LIT
11915	5793 ± 43	4.45 ± 0.06	−0.050 ± 0.021	8.615 ± 0.008	0.649 ± 0.004	0.134 ± 0.004	0.354 ± 0.004	0.699 ± 0.004	2	SAAO+LIT
12186	5812 ± 34	4.09 ± 0.05	0.094 ± 0.040	5.785 ± 0.006	0.654 ± 0.007	0.180 ± 0.028	0.360 ± 0.010	0.700 ± 0.010	0	LIT
14614	5803 ± 28	4.47 ± 0.03	−0.104 ± 0.016	7.840 ± 0.010	0.620 ± 0.010	0.130 ± 0.010	...	...	0	LIT
14632	6026 ± 42	4.28 ± 0.05	0.136 ± 0.019	4.047 ± 0.008	0.595 ± 0.007	0.118 ± 0.010	...	...	0	LIT
15457	5771 ± 65	4.56 ± 0.02	0.078 ± 0.041	4.836 ± 0.010	0.679 ± 0.007	0.188 ± 0.008	0.384 ± 0.005	0.726 ± 0.008	0	LIT
18261	5891 ± 34	4.44 ± 0.05	0.002 ± 0.016	7.980 ± 0.027	0.628 ± 0.006	0.083 ± 0.017	0.327 ± 0.047	0.670 ± 0.028	1	SPM+LIT
22263	5826 ± 48	4.54 ± 0.01	0.005 ± 0.029	5.497 ± 0.012	0.632 ± 0.012	0.136 ± 0.007	0.359 ± 0.005	0.691 ± 0.005	0	LIT
22528	5683 ± 52	4.33 ± 0.10	−0.350 ± 0.035	9.540 ± 0.010	0.630 ± 0.010	0.090 ± 0.010	...	...	0	LIT
23835	5723 ± 33	4.16 ± 0.05	−0.184 ± 0.017	4.920 ± 0.034	0.645 ± 0.005	0.142 ± 0.006	...	...	0	LIT
25670	5755 ± 37	4.38 ± 0.05	0.071 ± 0.017	8.275 ± 0.021	0.659 ± 0.004	0.167 ± 0.012	0.341 ± 0.036	0.698 ± 0.024	1	SPM+LIT
28336	5713 ± 61	4.53 ± 0.08	−0.170 ± 0.027	8.998 ± 0.001	0.654 ± 0.007	0.108 ± 0.019	0.354 ± 0.007	0.704 ± 0.010	2	SPM+SAAO+LIT
29525	5715 ± 61	4.41 ± 0.04	−0.005 ± 0.036	6.442 ± 0.014	0.660 ± 0.015	0.160 ± 0.004	...	...	0	LIT
30037	5690 ± 30	4.42 ± 0.06	0.050 ± 0.030	9.162 ± 0.015	0.682 ± 0.015	0.213 ± 0.015	0.361 ± 0.015	0.706 ± 0.015	1	SAAO
30502	5745 ± 25	4.47 ± 0.05	−0.010 ± 0.020	8.667 ± 0.015	0.664 ± 0.015	0.152 ± 0.015	0.368 ± 0.015	0.707 ± 0.015	1	SAAO
36512	5740 ± 15	4.50 ± 0.03	−0.092 ± 0.020	7.729 ± 0.011	0.656 ± 0.004	0.121 ± 0.004	0.356 ± 0.005	0.696 ± 0.004	3	SPM+SAAO
38072	5839 ± 68	4.53 ± 0.11	0.060 ± 0.037	9.222 ± 0.002	0.648 ± 0.004	0.147 ± 0.009	0.362 ± 0.005	0.701 ± 0.004	4	SPM+SAAO
38228	5693 ± 58	4.52 ± 0.07	0.007 ± 0.025	6.900 ± 0.010	0.682 ± 0.004	...	...	...	0	LIT
39748	5835 ± 30	4.48 ± 0.06	−0.200 ± 0.030	8.592 ± 0.009	0.615 ± 0.004	0.050 ± 0.004	0.340 ± 0.023	0.681 ± 0.004	4	SAAO+OPD
41317	5724 ± 15	4.46 ± 0.03	−0.044 ± 0.020	7.807 ± 0.004	0.668 ± 0.004	0.158 ± 0.004	0.365 ± 0.005	0.712 ± 0.008	3	SPM+SAAO+LIT
42438	5864 ± 47	4.46 ± 0.09	−0.052 ± 0.026	5.631 ± 0.009	0.619 ± 0.004	0.070 ± 0.004	...	...	0	LIT
43190	5775 ± 30	4.37 ± 0.06	0.120 ± 0.030	8.508 ± 0.015	0.670 ± 0.015	0.232 ± 0.015	0.370 ± 0.015	0.696 ± 0.015	1	SAAO
44324	5934 ± 49	4.51 ± 0.06	−0.020 ± 0.019	7.943 ± 0.010	0.620 ± 0.027	0.083 ± 0.035	0.321 ± 0.011	0.674 ± 0.016	4	SPM
44713	5784 ± 35	4.36 ± 0.03	0.096 ± 0.024	7.306 ± 0.006	0.668 ± 0.005	0.201 ± 0.006	0.371 ± 0.005	0.713 ± 0.005	0	LIT
44935	5800 ± 25	4.41 ± 0.05	0.070 ± 0.020	8.739 ± 0.014	0.645 ± 0.004	0.200 ± 0.007	0.344 ± 0.004	0.690 ± 0.004	2	SPM+SAAO
44997	5782 ± 29	4.52 ± 0.04	0.033 ± 0.020	8.347 ± 0.023	0.659 ± 0.008	0.202 ± 0.005	0.348 ± 0.008	0.698 ± 0.014	2	SPM+SAAO
46066	5709 ± 65	4.49 ± 0.12	−0.070 ± 0.039	8.928 ± 0.007	0.664 ± 0.017	0.188 ± 0.016	0.360 ± 0.008	0.717 ± 0.008	2	SPM
46126	5890 ± 30	4.48 ± 0.06	0.140 ± 0.030	8.514 ± 0.006	0.651 ± 0.004	0.149 ± 0.030	0.354 ± 0.006	0.704 ± 0.023	2	SAAO+LIT
49572	5831 ± 52	4.33 ± 0.06	0.010 ± 0.021	9.288 ± 0.006	0.640 ± 0.007	0.138 ± 0.006	0.336 ± 0.008	0.702 ± 0.007	1	SPM
49756	5804 ± 52	4.45 ± 0.07	0.041 ± 0.023	7.540 ± 0.008	0.647 ± 0.004	0.185 ± 0.004	0.343 ± 0.004	0.687 ± 0.007	4	SPM+SAAO+OPD+LIT
51258	5720 ± 25	4.23 ± 0.05	0.360 ± 0.030	7.874 ± 0.004	0.725 ± 0.004	0.344 ± 0.008	0.386 ± 0.006	0.735 ± 0.004	2	SAAO+LIT
52137	5842 ± 69	4.56 ± 0.08	0.070 ± 0.026	8.640 ± 0.010	0.640 ± 0.010	0.190 ± 0.010	...	...	0	LIT
53721	5916 ± 53	4.48 ± 0.01	0.027 ± 0.038	5.049 ± 0.015	0.606 ± 0.010	0.124 ± 0.007	...	...	0	LIT
54102	5870 ± 30	4.51 ± 0.06	0.040 ± 0.030	8.653 ± 0.004	0.649 ± 0.004	0.142 ± 0.015	0.346 ± 0.004	0.698 ± 0.004	2	SAAO

Table 5
(Continued)

HIP	$T_{\rm eff}$ (K)	$\log g$	[Fe/H]	V	$(B-V)$	$(U-B)$	$(V-R)$	$(V-I)$	$N_{\rm obs}$[a]	Source[b]
55409	5760 ± 25	4.52 ± 0.05	−0.010 ± 0.020	8.002 ± 0.014	0.659 ± 0.004	0.193 ± 0.011	0.368 ± 0.004	0.719 ± 0.004	5	SAAO+OPD+LIT
55459	5838 ± 21	4.42 ± 0.03	0.038 ± 0.012	7.646 ± 0.004	0.644 ± 0.004	0.147 ± 0.010	0.338 ± 0.006	0.692 ± 0.006	1	SPM+LIT
56948	5795 ± 23	4.43 ± 0.03	0.023 ± 0.014	8.669 ± 0.004	0.646 ± 0.006	0.180 ± 0.006	0.339 ± 0.006	0.680 ± 0.006	1	SPM
56997	5559 ± 65	4.53 ± 0.08	−0.030 ± 0.027	5.321 ± 0.015	0.723 ± 0.013	0.261 ± 0.018	...	...	0	LIT
57291	5690 ± 22	4.30 ± 0.04	0.304 ± 0.030	7.466 ± 0.008	0.740 ± 0.004	0.354 ± 0.006	0.375 ± 0.016	0.732 ± 0.013	2	SAAO
59357	5810 ± 30	4.45 ± 0.06	−0.240 ± 0.030	8.731 ± 0.039	0.618 ± 0.004	0.078 ± 0.004	0.351 ± 0.010	0.715 ± 0.031	6	SPM+SAAO+OPD+LIT
59610	5899 ± 62	4.34 ± 0.04	−0.034 ± 0.041	7.360 ± 0.010	0.640 ± 0.010	...	...	...	0	LIT
60081	5811 ± 21	4.38 ± 0.04	0.315 ± 0.030	8.023 ± 0.007	0.696 ± 0.006	0.290 ± 0.008	0.373 ± 0.007	0.702 ± 0.007	2	SAAO
60314	5874 ± 72	4.52 ± 0.10	0.110 ± 0.033	8.780 ± 0.008	0.649 ± 0.017	0.155 ± 0.007	0.337 ± 0.011	0.676 ± 0.009	1	SPM+LIT
60370	5897 ± 25	4.46 ± 0.05	0.171 ± 0.030	6.703 ± 0.004	0.641 ± 0.005	0.148 ± 0.013	0.349 ± 0.008	0.674 ± 0.008	2	SAAO+LIT
60653	5725 ± 30	4.38 ± 0.06	−0.290 ± 0.030	8.735 ± 0.005	0.638 ± 0.014	0.109 ± 0.015	0.360 ± 0.004	0.702 ± 0.010	4	SAAO+OPD
62175	5849 ± 51	4.43 ± 0.06	0.140 ± 0.021	8.011 ± 0.005	0.661 ± 0.004	0.194 ± 0.007	0.345 ± 0.006	0.682 ± 0.006	1	SPM+LIT
64150	5755 ± 41	4.39 ± 0.05	0.056 ± 0.016	6.822 ± 0.061	0.676 ± 0.020	0.204 ± 0.004	0.374 ± 0.013	0.700 ± 0.012	3	SPM+SAAO+LIT
64497	5860 ± 110	4.56 ± 0.11	0.120 ± 0.037	8.978 ± 0.057	0.668 ± 0.022	0.182 ± 0.008	0.362 ± 0.009	0.687 ± 0.004	6	SPM+SAAO+OPD
64713	5815 ± 25	4.52 ± 0.05	−0.010 ± 0.020	9.260 ± 0.022	0.649 ± 0.004	0.140 ± 0.010	0.351 ± 0.023	0.710 ± 0.019	5	SPM+SAAO+OPD
64794	5743 ± 61	4.33 ± 0.08	−0.100 ± 0.027	8.428 ± 0.041	0.637 ± 0.006	0.141 ± 0.008	0.344 ± 0.028	0.701 ± 0.013	6	SPM+SAAO+OPD+LIT
64993	5875 ± 30	4.56 ± 0.06	0.090 ± 0.030	8.900 ± 0.022	0.656 ± 0.008	0.166 ± 0.008	0.348 ± 0.013	0.706 ± 0.009	4	SPM+SAAO+OPD
66618	5951 ± 25	4.35 ± 0.05	0.135 ± 0.030	6.962 ± 0.004	0.622 ± 0.004	0.175 ± 0.005	...	...	0	LIT
66885	5685 ± 30	4.48 ± 0.06	−0.380 ± 0.030	9.302 ± 0.014	0.635 ± 0.004	0.077 ± 0.014	0.364 ± 0.014	0.730 ± 0.005	4	SPM+SAAO+OPD+LIT
69063	5670 ± 30	4.31 ± 0.06	−0.450 ± 0.030	8.882 ± 0.006	0.623 ± 0.004	0.068 ± 0.004	0.352 ± 0.004	0.706 ± 0.010	2	SAAO+LIT
71683	5840 ± 22	4.33 ± 0.04	0.228 ± 0.030	0.002 ± 0.008	0.653 ± 0.023	0.230 ± 0.004	0.362 ± 0.010	0.693 ± 0.010	0	LIT
72659	5517 ± 67	4.56 ± 0.09	−0.117 ± 0.033	4.718 ± 0.008	0.748 ± 0.019	0.231 ± 0.019	...	...	0	LIT
73815	5803 ± 33	4.34 ± 0.05	0.020 ± 0.016	8.174 ± 0.003	0.663 ± 0.006	0.164 ± 0.005	0.352 ± 0.009	0.696 ± 0.006	5	SPM+SAAO+OPD+LIT
74341	5853 ± 57	4.51 ± 0.08	0.090 ± 0.026	8.860 ± 0.013	0.673 ± 0.013	0.165 ± 0.018	0.348 ± 0.010	0.689 ± 0.007	6	SPM+OPD
74389	5859 ± 24	4.48 ± 0.04	0.105 ± 0.030	7.773 ± 0.014	0.636 ± 0.014	0.153 ± 0.014	0.349 ± 0.004	0.687 ± 0.005	6	SPM+SAAO+OPD
75923	5775 ± 25	4.56 ± 0.05	−0.020 ± 0.020	9.156 ± 0.012	0.658 ± 0.006	0.137 ± 0.004	0.353 ± 0.013	0.704 ± 0.015	6	SPM+SAAO+OPD
77052	5697 ± 33	4.54 ± 0.02	0.035 ± 0.023	5.868 ± 0.011	0.686 ± 0.011	0.234 ± 0.010	0.380 ± 0.010	0.740 ± 0.010	0	LIT
77466	5700 ± 56	4.40 ± 0.09	−0.280 ± 0.028	9.204 ± 0.009	0.647 ± 0.005	0.120 ± 0.014	...	...	0	LIT
77740	5900 ± 19	4.45 ± 0.04	0.125 ± 0.030	...	0.628 ± 0.012	...	...	...	0	LIT
77883	5695 ± 25	4.39 ± 0.05	0.040 ± 0.020	8.755 ± 0.020	0.687 ± 0.008	0.224 ± 0.005	0.371 ± 0.004	0.729 ± 0.014	6	SPM+SAAO+OPD
78028	5879 ± 98	4.57 ± 0.12	−0.030 ± 0.041	8.651 ± 0.012	0.638 ± 0.019	0.118 ± 0.024	0.334 ± 0.016	0.683 ± 0.016	5	SPM
78680	5923 ± 67	4.57 ± 0.08	−0.000 ± 0.027	8.243 ± 0.013	0.626 ± 0.018	0.079 ± 0.021	0.337 ± 0.016	0.698 ± 0.016	3	SPM
79186	5709 ± 48	4.27 ± 0.08	−0.120 ± 0.024	8.341 ± 0.014	0.676 ± 0.004	0.140 ± 0.033	0.356 ± 0.022	0.724 ± 0.018	3	SPM+LIT
79304	5945 ± 30	4.53 ± 0.06	0.110 ± 0.030	8.703 ± 0.021	0.646 ± 0.015	0.160 ± 0.009	0.347 ± 0.004	0.683 ± 0.008	7	SPM+SAAO+OPD
79578	5860 ± 33	4.53 ± 0.07	0.072 ± 0.030	6.533 ± 0.033	0.647 ± 0.007	0.145 ± 0.012	0.352 ± 0.008	0.699 ± 0.004	2	SAAO+LIT
79672	5822 ± 9	4.45 ± 0.02	0.051 ± 0.020	5.510 ± 0.009	0.650 ± 0.004	0.177 ± 0.004	0.357 ± 0.005	0.691 ± 0.011	3	SPM+SAAO+LIT
80337	5881 ± 33	4.53 ± 0.02	0.033 ± 0.022	5.391 ± 0.012	0.628 ± 0.011	0.108 ± 0.048	0.353 ± 0.005	0.681 ± 0.006	0	LIT
81512	5790 ± 58	4.46 ± 0.07	−0.020 ± 0.025	9.245 ± 0.015	0.652 ± 0.017	0.140 ± 0.019	0.353 ± 0.019	0.712 ± 0.016	3	SPM
82853	5640 ± 30	4.21 ± 0.06	−0.180 ± 0.030	8.965 ± 0.163	0.660 ± 0.007	0.181 ± 0.004	0.396 ± 0.004	0.729 ± 0.008	3	SAAO+OPD
83601	6071 ± 43	4.38 ± 0.08	0.048 ± 0.028	6.013 ± 0.008	0.575 ± 0.005	0.041 ± 0.012	0.325 ± 0.010	0.635 ± 0.010	0	LIT
83707	5880 ± 30	4.45 ± 0.06	0.150 ± 0.030	8.605 ± 0.011	0.655 ± 0.004	0.181 ± 0.004	0.350 ± 0.004	0.699 ± 0.004	3	SAAO+OPD
85042	5692 ± 37	4.39 ± 0.02	0.037 ± 0.026	6.287 ± 0.004	0.679 ± 0.004	0.233 ± 0.008	0.364 ± 0.020	0.707 ± 0.051	2	SAAO+LIT
85272	5700 ± 30	4.42 ± 0.06	−0.340 ± 0.030	9.121 ± 0.000	0.632 ± 0.016	0.095 ± 0.012	0.363 ± 0.009	0.717 ± 0.006	3	SAAO+OPD
85285	5730 ± 30	4.43 ± 0.06	−0.390 ± 0.030	8.365 ± 0.015	0.629 ± 0.011	0.065 ± 0.013	0.348 ± 0.009	0.712 ± 0.008	7	SPM+SAAO+OPD
86796	5809 ± 22	4.28 ± 0.04	0.298 ± 0.030	5.124 ± 0.006	0.700 ± 0.004	0.240 ± 0.004	0.385 ± 0.004	0.708 ± 0.004	2	SAAO+LIT
88194	5735 ± 21	4.40 ± 0.03	−0.071 ± 0.010	7.101 ± 0.035	0.639 ± 0.008	0.126 ± 0.004	0.360 ± 0.006	0.712 ± 0.008	5	SPM+OPD+LIT
88427	5810 ± 57	4.42 ± 0.07	−0.160 ± 0.025	9.329 ± 0.006	0.638 ± 0.013	0.089 ± 0.022	0.336 ± 0.018	0.704 ± 0.007	1	SPM

Table 5
(Continued)

HIP	$T_{\rm eff}$ (K)	$\log g$	[Fe/H]	V	$(B-V)$	$(U-B)$	$(V-R)$	$(V-I)$	$N_{\rm obs}$[a]	Source[b]
89162	5835 ± 30	4.32 ± 0.06	0.070 ± 0.030	8.902 ± 0.005	0.658 ± 0.005	0.176 ± 0.004	0.360 ± 0.006	0.696 ± 0.006	4	SAAO+OPD
89443	5796 ± 73	4.48 ± 0.12	-0.020 ± 0.038	8.843 ± 0.004	0.660 ± 0.007	0.147 ± 0.013	0.359 ± 0.006	0.715 ± 0.006	1	SPM
89650	5855 ± 25	4.48 ± 0.05	0.020 ± 0.020	8.944 ± 0.001	0.643 ± 0.004	0.126 ± 0.004	0.356 ± 0.004	0.688 ± 0.009	7	SAAO+OPD
91332	5775 ± 25	4.20 ± 0.05	0.206 ± 0.030	7.971 ± 0.008	0.692 ± 0.007	0.263 ± 0.004	0.365 ± 0.015	0.705 ± 0.004	2	SAAO+LIT
96402	5713 ± 49	4.33 ± 0.03	-0.029 ± 0.030	7.560 ± 0.010	0.678 ± 0.007	0.154 ± 0.010	...	...	0	LIT
96895	5808 ± 39	4.33 ± 0.05	0.097 ± 0.020	5.959 ± 0.009	0.644 ± 0.006	0.189 ± 0.009	...	...	0	LIT
96901	5737 ± 28	4.34 ± 0.04	0.055 ± 0.016	6.228 ± 0.019	0.663 ± 0.005	0.191 ± 0.016	...	...	0	LIT
100963	5802 ± 17	4.45 ± 0.03	0.008 ± 0.013	7.089 ± 0.021	0.651 ± 0.013	0.128 ± 0.024	0.342 ± 0.004	0.703 ± 0.007	3	SPM+OPD
100970	5823 ± 40	4.23 ± 0.03	0.083 ± 0.025	6.895 ± 0.015	0.645 ± 0.005	0.180 ± 0.020	...	...	0	LIT
109110	5817 ± 60	4.46 ± 0.03	0.062 ± 0.030	7.570 ± 0.010	0.674 ± 0.015	...	...	...	0	LIT
102152	5737 ± 47	4.35 ± 0.06	-0.010 ± 0.022	9.208 ± 0.015	0.669 ± 0.004	0.176 ± 0.019	0.382 ± 0.004	0.726 ± 0.004	3	SPM+SAAO
104504	5836 ± 48	4.50 ± 0.06	-0.160 ± 0.022	8.544 ± 0.021	0.622 ± 0.004	0.068 ± 0.012	0.363 ± 0.004	0.701 ± 0.004	5	SPM+SAAO+OPD+LIT
107350	6015 ± 50	4.48 ± 0.07	-0.020 ± 0.019	5.942 ± 0.011	0.587 ± 0.004	0.032 ± 0.004	...	...	0	LIT
108708	5875 ± 51	4.51 ± 0.07	0.150 ± 0.024	8.939 ± 0.003	0.659 ± 0.004	0.162 ± 0.012	0.368 ± 0.004	0.711 ± 0.004	4	SPM+OPD
108996	5838 ± 56	4.50 ± 0.08	0.060 ± 0.027	8.881 ± 0.012	0.648 ± 0.008	0.152 ± 0.025	0.351 ± 0.011	0.691 ± 0.011	6	SPM+SAAO+OPD
109931	5739 ± 74	4.29 ± 0.08	0.040 ± 0.026	8.956 ± 0.019	0.663 ± 0.006	0.194 ± 0.016	0.367 ± 0.034	0.710 ± 0.020	1	SPM+LIT
113357	5803 ± 47	4.38 ± 0.05	0.221 ± 0.017	5.467 ± 0.020	0.665 ± 0.012	0.233 ± 0.028	...	...	0	LIT
118159	5905 ± 44	4.55 ± 0.07	-0.010 ± 0.022	9.010 ± 0.006	0.627 ± 0.004	0.090 ± 0.004	0.341 ± 0.007	0.680 ± 0.004	4	SPM+SAAO+OPD

Notes.

[a] Number of photometric observations made in this work.

[b] If the source includes LIT, which corresponds to previously published values, the LIT flag applies only to the *UBV* data. The $RI_{\rm (C)}$ data are, to the best of our knowledge, published here for the first time, except for stars with the following HIP numbers: 1499, 11072, 12186, 15457, 22263, 41317, 44713, 71683, 77052, 79672, 80337, 83601, and 86796.

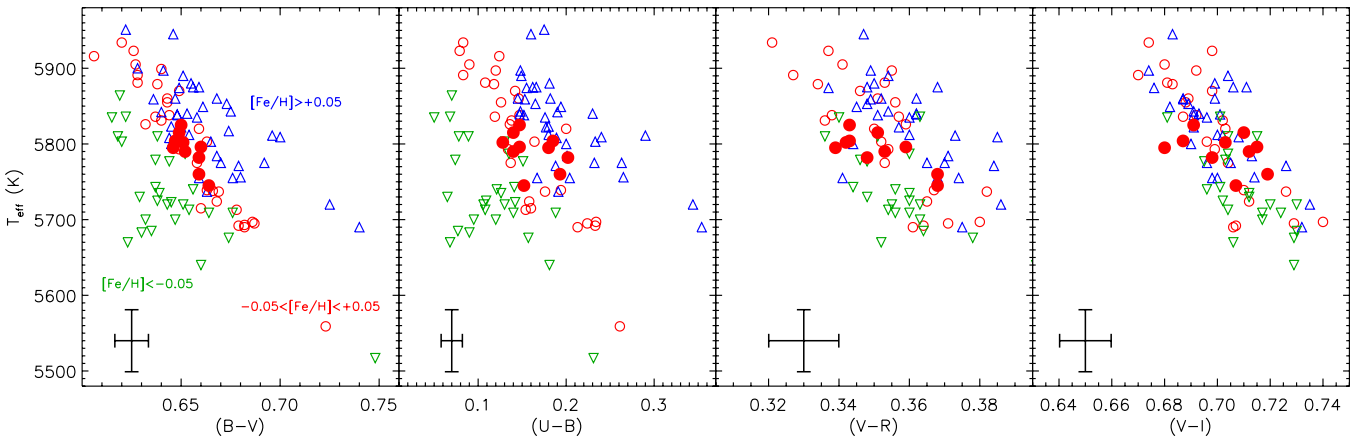

Figure 4. Effective temperature vs. color relations for our sample of solar twins and analogs. Open circles represent stars with near solar metallicity ($-0.05 <$ [Fe/H] $< +0.05$). Upside-down and regular triangles correspond to stars with [Fe/H] < -0.05 and [Fe/H] $> +0.05$, respectively. Our sample of solar twin stars is shown with filled circles. Average error bars are shown at bottom left of each panel.

(A color version of this figure is available in the online journal.)

3. THE SOLAR COLORS

3.1. Color–$T_{\rm eff}$ Relations

As is well known, colors are good indicators of $T_{\rm eff}$, although in many cases they can also be sensitive to other stellar parameters. Figure 4, for example, shows the relation between our $UBV(RI)_{\rm C}$ colors and $T_{\rm eff}$, which clearly reveals a dependence on a second parameter, namely [Fe/H], although this is much more pronounced for $(B - V)$ than $(V - I)$. The sensitivity of the $UBV(RI)_{\rm C}$ colors to $\log g$ is very weak, as will be shown quantitatively later in this section. As noted in Section 2, the $T_{\rm eff}$, $\log g$, and [Fe/H] values we used were derived from our high-quality spectra, using the standard excitation/ionization equilibrium balance condition for Fe I and Fe II lines (e.g., Ramírez et al. 2009). Although this technique is heavily model dependent, the fact that our sample stars are all very similar to our Sun allows us to minimize the impact of systematic errors because they are nearly the same for all of these objects and because we employ a strictly differential analysis using the solar spectrum as reference.

We used the data from Table 5 to perform a multiple linear regression of the following form:

$$\text{color} = a_0 + a_1(T_{\rm eff} - 5777\ \text{K}) + a_1(\log g - 4.44) + a_2[\text{Fe/H}]\ , \quad (1)$$

from which the solar colors are inferred: $\text{color}_\odot = a_0$. The error in the solar color is derived by adding in quadrature the 1σ scatter of the regression, which takes into account the errors in the observed stellar colors and the error due to the stellar parameter uncertainties. To calculate the error due to $T_{\rm eff}$, $\log g$, and [Fe/H] uncertainties, we computed 5000 solar colors using $T_{\rm eff}$, $\log g$, and [Fe/H] values modified randomly from their mean values, assuming a Gaussian distribution for each of the three stellar atmospheric parameters. The individual errors in these parameters for each star, as listed in Table 5, were adopted as the standard deviations of these distributions. The 1σ scatter from the 5000 tests described above was finally adopted as the uncertainty due to errors in the stellar parameters.

Two sets of solar colors were derived: the first one using the entire sample of 112 solar analogs and the second set inferred using only the data for the 10 stars that most closely resemble the Sun (hereafter referred to as the solar twins). The solar twin sample was defined as those stars having their stellar parameters $T_{\rm eff}$, $\log g$, and [Fe/H] within 1.4σ from the solar values, where σ is the average error in the stellar parameters of the sample. Modifying slightly the definition of solar twin star has little impact on our results. The multiplicative factor of 1.4 was chosen arbitrarily so that the sample of solar twins could have exactly 10 elements.

Table 6
Solar Colors Inferred from $T_{\rm eff}$ and [Fe/H] Measurements

Color	Solar Twins	Solar Analogs
$(B - V)$	0.653 ± 0.005	0.658 ± 0.014
$(U - B)$	0.166 ± 0.022	0.163 ± 0.026
$(V - R)$	0.352 ± 0.007	0.361 ± 0.011
$(V - I)$	0.702 ± 0.010	0.707 ± 0.012

The solar colors derived using the method described above are listed in Table 6. In particular, we find $(B - V)_\odot = 0.653 \pm 0.005$ using only the solar twin data. This value is consistent within the 1σ errors with that derived using the entire sample of solar analogs, $(B - V)_\odot = 0.658 \pm 0.014$. We note, however, that the mean $(B - V)_\odot$ value increases by 0.005 mag when using the full sample, which suggests that the effective temperatures of non-solar twin stars may be slightly overestimated, making the Sun appear redder than it actually is. We find that the mean $(B - V)_\odot$ value obtained using only solar twins would be in perfect agreement with that derived using the full sample if the $T_{\rm eff}$ values of non-solar twin stars were cooler by about 20 K. This implies that systematic errors in the model-dependent determination of stellar parameters from iron line analysis (excitation/ionization equilibrium), although small, are non-negligible for solar analogs, but not so important for the solar twins. This is of course true only when dealing with very high quality spectroscopic data such as those used by Meléndez et al. (2009), Ramírez et al. (2009), and Baumann et al. (2010), where effective temperatures with a precision comparable to 20 K are possible to achieve.

The $(U - B)_\odot$ color has the largest error of all $UBV(RI)_{\rm C}$ solar colors derived; it is greater than 0.02 mag. This is not at all surprising because U-filter observations and their standardization are known to be very challenging. For $(V - R)$ and $(V - I)$ we derive solar colors with errors below or about 0.01 mag. As with $(B - V)$, the solar $(V - R)$ and $(V - I)$ colors inferred using solar twins are slightly bluer than those

obtained using the full sample of solar analogs. Decreasing the $T_{\rm eff}$ values of non-solar twin stars by 20 K gives agreement within 0.001 mag for the mean $(V-I)_{\odot}$ values, but the $(V-R)_{\odot}$ colors still differ by 0.007 mag. A $T_{\rm eff}$ decrease of about 70 K is necessary to make the $(V-R)_{\odot}$ colors agree perfectly. This is highly unlikely given the high precision of our $T_{\rm eff}$ determinations, and therefore suggests that there are small systematic errors affecting our $(V-R)$ colors.

Even though $\log g$ is included in the regression formula (Equation (1)) for completeness, we find that the precision of our results is not compromised if we choose to neglect it. For example, a regression using only $T_{\rm eff}$ and [Fe/H] gives us the same solar $(B-V)$ colors of solar twins or analogs within 0.001 mag. Moreover, the errors are identical to the case when $\log g$ is also included. This is likely the result of having selected only main-sequence stars for our sample. The impact of [Fe/H] on these calculations, however, must not be ignored. A regression on $T_{\rm eff}$ only, or even $T_{\rm eff}$ and $\log g$, results in a solar $(B-V)$ color with an error that is about twice as large as that obtained using Equation (1). As mentioned earlier, the metallicity dependence of $UBV(RI)_{\rm C}$ colors is clearly seen in Figure 4. We also tested regression formulas including quadratic terms, i.e., $T_{\rm eff}^2$, $[{\rm Fe/H}]^2$, and $\log g^2$, as well as mixed terms such as $T_{\rm eff} \times [{\rm Fe/H}]$, but found no noticeable improvements; the 1σ scatter of the regression (i.e., data minus fit value residuals) did not change by more than 0.001 mag, and the same was true for the mean values obtained for the solar colors.

3.2. Spectral-line–Depth Ratios

The strength of a spectral line depends on many parameters. In addition to the physical conditions of the gas in which the line is formed, which makes the line strength sensitive to the model atmosphere adopted, the properties of the atom, ion, or molecule responsible for the absorption and those of the transition that produces the line are all directly related to the line strength. Of particular interest for our work is the excitation potential (EP) of the feature. Spectral lines with very different EP values show significantly different sensitivity to $T_{\rm eff}$. Thus, ratios of depths of spectral line pairs with very different EP values are known to be excellent $T_{\rm eff}$ indicators (e.g., Gray & Johanson 1991; Gray 1994), and therefore they are expected to correlate well with observed colors.

Gray (1992) was the first to use line–depth ratios (LDRs) to infer solar colors. As pointed out by him, one of the great advantages of using LDRs is that they are nearly insensitive to the stellar metallicity, at least for nearby thin-disk stars, because, to first approximation, the line strengths scale with [Fe/H] regardless of the element producing the line. If, in addition, the line pairs have similar wavelengths and the spectroscopic data used are very homogeneous, particularly concerning the continuum normalization, LDRs are also independent of spectral resolution. Using LDRs to infer the solar colors also has the great advantage of being a completely model-independent approach.

We used our high-resolution, high signal-to-noise ratio spectra to measure as many LDRs as possible for all line pairs listed in the study by Kovtyukh et al. (2003) and inspected the LDR versus color relations obtained using our photometric data. We fitted a straight line to each of these relations and computed the standard deviation (1σ) of the fit minus data residuals. Two examples of these fits are shown in Figure 5. Then we measured the LDRs in our solar spectra, which are in fact reflected Sun-light observations of bright asteroids, and used the LDR versus color fits to infer a solar color for each line pair. The

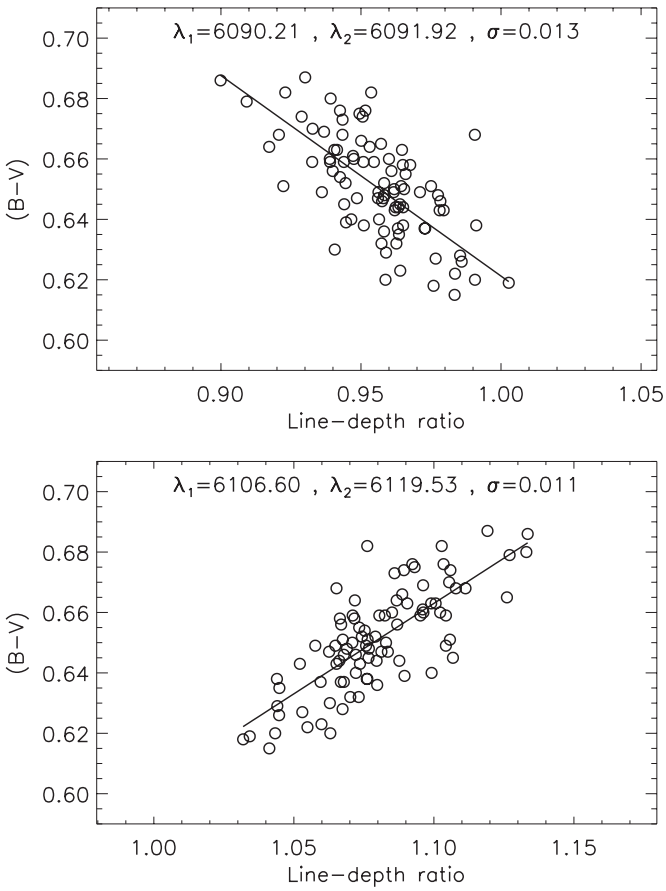

Figure 5. Two examples of observed $(B-V)$ color as a function of line–depth ratio measured in our spectra. The wavelengths of the lines used and the 1σ of the linear fit shown with a solid line are given in the upper part of each panel.

weighted mean and average values obtained from all line pairs used were adopted as the final solar colors. Not all line pairs listed in the Kovtyukh et al. (2003) study were used in the end. Line pairs for which the linear fits had a 1σ value with a significant contribution from observational errors in the spectra were discarded. For example, for $(B-V)$ we excluded the fits with $1\sigma > 0.015$ mag because the typical $(B-V)$ error is 0.01 mag, and adopting only the pairs with $1\sigma < 0.015$ mag implies that the only pairs that are used are those in which the spectroscopic errors (i.e., the errors in LDR), when propagated to the photometric data in this relation, are similar to the photometric ones or smaller. Although somewhat arbitrary, this automated procedure eliminates line pairs which may be affected by blends, continuum normalization issues intrinsic to our data, and/or instrumental imperfections.

As an example, in Table 7 we list all the line pairs used to derive the solar $(B-V)$ color from LDR versus color relations. For each pair, we provide the number of stars, $N_{\star}$, used to construct the empirical relation and the standard deviation of the fit minus data residuals ($\sigma_{\rm fit}$). Also, for each pair we provide the mean and standard deviation of the $(B-V)$ color that corresponds to the nine reflected Sun-light asteroid observations used for solar reference ($\sigma_{\rm ss}$). This is because each solar spectrum gives us a slightly different value for the LDR of each pair. Note that the standard deviation from the mean color of our nine solar spectra is very small; in many cases it is below 0.005 mag. The weighted mean and sample variance of the $(B-V)$ solar colors inferred from the 45 line pairs used

Table 7
$(B-V)_\odot$ Color Inferred from LDR Measurements

λ_1 (Å)	Species	λ_2 (Å)	Species	$N_\star$	$\sigma_{\rm fit}$	$(B-V)_\odot$	$\sigma_{\rm ss}$
5490.15	Ti I	5517.53	Si I	90	0.014	0.649	0.005
5690.43	Si I	5727.05	V I	90	0.015	0.649	0.006
5701.11	Si I	5727.05	V I	90	0.012	0.651	0.006
5727.05	V I	5753.65	Si I	90	0.015	0.653	0.002
6007.31	Ni I	6046.00	S I	90	0.013	0.654	0.005
6039.73	V I	6046.00	S I	90	0.014	0.645	0.006
6039.73	V I	6052.68	S I	90	0.013	0.654	0.004
6046.00	S I	6062.89	Fe I	90	0.012	0.651	0.005
6046.00	S I	6085.27	Fe I	42	0.011	0.652	0.007
6046.00	S I	6091.18	Ti I	90	0.015	0.645	0.006
6052.68	S I	6062.89	Fe I	90	0.012	0.656	0.003
6052.68	S I	6081.44	V I	34	0.014	0.654	0.005
6052.68	S I	6091.18	Ti I	90	0.014	0.652	0.004
6090.21	V I	6091.92	Si I	90	0.013	0.655	0.004
6090.21	V I	6106.60	Si I	90	0.011	0.657	0.004
6090.21	V I	6125.03	Si I	90	0.013	0.654	0.003
6090.21	V I	6131.86	Si I	83	0.012	0.656	0.006
6091.92	Si I	6128.99	Ni I	90	0.014	0.657	0.006
6106.60	Si I	6119.53	V I	90	0.011	0.656	0.004
6106.60	Si I	6126.22	Ti I	90	0.013	0.653	0.003
6106.60	Si I	6135.36	V I	89	0.014	0.653	0.005
6108.12	Ni I	6155.14	Si I	90	0.015	0.656	0.003
6119.53	V I	6131.86	Si I	83	0.014	0.651	0.006
6125.03	Si I	6128.99	Ni I	90	0.014	0.656	0.002
6128.99	Ni I	6131.86	Si I	83	0.013	0.658	0.007
6175.42	Ni I	6224.51	V I	84	0.015	0.655	0.003
6176.81	Ni I	6224.51	V I	84	0.015	0.655	0.003
6186.74	Ni I	6224.51	V I	32	0.014	0.656	0.004
6199.19	V I	6215.15	Fe I	74	0.015	0.656	0.004
6204.64	Ni I	6224.51	V I	84	0.015	0.655	0.002
6204.64	Ni I	6243.11	V I	90	0.013	0.649	0.003
6215.15	Fe I	6224.51	V I	84	0.013	0.655	0.003
6215.15	Fe I	6251.82	V I	90	0.015	0.655	0.004
6223.99	Ni I	6224.51	V I	84	0.014	0.656	0.003
6223.99	Ni I	6243.11	V I	89	0.014	0.648	0.006
6224.51	V I	6230.09	Ni I	84	0.014	0.655	0.004
6230.09	Ni I	6243.11	V I	90	0.013	0.651	0.005
6240.66	Fe I	6243.81	Si I	90	0.014	0.654	0.010
6240.66	Fe I	6244.48	Si I	90	0.014	0.654	0.008
6243.11	V I	6243.81	Si I	90	0.015	0.649	0.002
6327.60	Ni I	6414.99	Si I	35	0.013	0.655	0.005
6414.99	Si I	6498.95	Fe I	35	0.013	0.651	0.007
6710.31	Fe I	6748.84	S I	89	0.012	0.651	0.006
6710.31	Fe I	6757.17	S I	90	0.012	0.650	0.007
6757.17	S I	6806.85	Fe I	34	0.011	0.656	0.005

are finally adopted as the solar color. We used as weights (w) the inverse of the standard deviations of the LDR versus color fits and the 1σ scatter in the colors obtained for the nine solar spectra, added in quadrature, i.e., $1/w = \sigma_{\rm fit}^2 + \sigma_{\rm ss}^2$ (see Table 7).

Some of the scatter seen in Figure 5 could in principle be attributed to [Fe/H] and/or $\log g$ effects. To test this hypothesis, we repeated the procedures described above, but using, instead of a simple linear fit of LDR versus color, a linear regression similar to Equation (1), replacing the ($T_{\rm eff} - 5777$ K) term with the LDR values. The exact same mean value and error were obtained for $(B-V)_\odot$, suggesting that the impact of [Fe/H] and $\log g$ on the LDR versus color relations is below the 0.001 mag level. This implies that the scatter seen in Figure 5 is dominated by observational errors in both LDR and $(B-V)$.

We computed solar colors for each line pair and for each solar spectrum available. Our spectra come from two different sources and were taken on several different observing runs. The results given in Table 7 were obtained using all available data. We made sure that analyzing the data separately per run or per observing site does not improve these results in a significant manner. In fact, due to the lower number of stars available to derive the solar colors, this approach typically gives us larger errors, in some cases about twice as large for $(B-V)$, for example. Thus, we conclude that small differences in the spectral resolution, sky conditions, and/or instrumental setup have a negligible impact in our derivation of the solar colors. This observation also suggests that the continuum normalization of all our available data is robust and consistent across different data sets as well as observing runs and sites.

Table 8
Solar Colors Inferred from LDR Measurements

Color	Value	$N_{\rm pairs}$
$(B-V)$	0.653 ± 0.003	45
$(U-B)$	0.158 ± 0.009	42
$(V-R)$	0.356 ± 0.003	47
$(V-I)$	0.701 ± 0.003	53

We performed a similar exercise to the one described above to derive the other $UBV(RI)_{\rm C}$ solar colors, which are listed in Table 8. Using the LDR technique, we find $(B-V)_\odot = 0.653 \pm 0.003$, $(U-B)_\odot = 0.158 \pm 0.009$, $(V-R)_\odot = 0.356 \pm 0.003$, and $(V-I) = 0.701 \pm 0.003$, in excellent agreement with the solar colors obtained with the method described in Section 3.1. The significantly smaller error bars obtained with the LDR method are probably due to the fact that no systematic uncertainties similar to those of the stellar atmospheric parameters affect the LDR measurements, in addition to the fact that the spectroscopic data are very homogeneous and of extremely high quality.

4. CONCLUSIONS

The problem of the lack of important photometric data for solar analog stars in the $UBV(RI)_{\rm C}$ system has been addressed and solved with our $UBV(RI)_{\rm C}$ observations of 80 stars very similar to our Sun for which previously obtained high resolution, high signal-to-noise ratio spectra are available. The combined use of high-quality photometric and spectroscopic data of Sun-like stars allows us to study the Sun as a star without the need to modify or design instruments specifically for the direct observation of the Sun.

We have derived the solar colors in the $UBV(RI)_{\rm C}$ system using two different methods. The first one uses the atmospheric parameters $T_{\rm eff}$, $\log g$, and [Fe/H] derived using a model-dependent analysis, whereas the second method employs only measurements of spectral LDRs and the observed photometry, thus being completely model-independent. We find excellent agreement for the solar colors derived using these two techniques. In particular, we derive $(B-V)_\odot = 0.653 \pm 0.005$, but the LDR method gives a smaller error of 0.003 mag. An uncertainty of 0.005 mag in $(B-V)_\odot$ translates into an error of ± 16 K in $T_{\rm eff}$ whereas a 0.003 mag uncertainty corresponds to only 9 K. Thus, our highly precise solar colors can be used to constrain stellar models and calibrate effective temperature scales or color–$T_{\rm eff}$ relations at the 10 K level.

With respect to the recent debate in the literature concerning the solar $(B-V)$ color, our results favor the "red" value closer to 0.65 mag over the "blue" solar color of about 0.62 mag. Given the high quality of our photometric and spectroscopic

data, as well as our careful sample selection and derivation of solar colors from the wealth of available data, we argue that our solar $UBV(RI)_C$ colors are the most precise and reliable ones published to date. Along with the solar *uvby*-β colors derived by Meléndez et al. (2010), precise and accurate solar colors in the historically most important photometric systems are now available.

I.R.'s work was performed under contract with the California Institute of Technology (Caltech) funded by NASA through the Sagan Fellowship Program. This paper uses observations made at the South African Astronomical Observatory (SAAO). J.M. acknowledges support from FAPESP (2010/17510-3), CNPq, and USP.

REFERENCES

Baumann, P., Ramírez, I., Meléndez, J., Asplund, M., & Lind, K. 2010, A&A, 519, A87
Bessell, M. S. 2005, ARA&A, 43, 293
Blackwell, D. E., Shallis, M. J., & Selby, M. J. 1979, MNRAS, 188, 847
Casagrande, L., Portinari, L., & Flynn, C. 2006, MNRAS, 373, 13
Casagrande, L., Ramírez, I., Meléndez, J., Bessell, M., & Asplund, M. 2010, A&A, 512, 54
Cayrel de Strobel, G. 1996, A&AR, 7, 243
Chmielewski, Y. 1981, A&A, 93, 334
Clements, G. L., & Neff, J. S. 1979, A&A, 75, 193
Cousins, A. W. J. 1976, Mem. R. Astron. Soc., 81, 25
Fukugita, M., Ichikawa, T., Gunn, J. E., et al. 1996, AJ, 111, 1748
Graham, J. A. 1982, PASP, 94, 244
Gray, D. F. 1992, PASP, 104, 1035
Gray, D. F. 1994, PASP, 106, 1248
Gray, D. F., & Johanson, H. L. 1991, PASP, 103, 439
Harris, W. E., Fitzgerald, M. P., & Reed, B. C. 1981, PASP, 93, 507
Holmberg, J., Flynn, C., & Portinari, L. 2006, MNRAS, 367, 449
Jablonski, F., Baptista, R., Barroso, J., et al. 1994, PASP, 106, 1172
Johnson, H. L., & Morgan, W. W. 1953, ApJ, 117, 313
Kilkenny, D., Balona, L. A., Carter, D. B., Ellis, D. T., & Woodhouse, G. F. W. 1988, Mon. Notes Astron. Soc. South. Afr., 47, 69
Kovtyukh, V. V., Soubiran, C., Belik, S. I., & Gorlova, N. I. 2003, A&A, 411, 559
Meléndez, J., Asplund, M., Gustafsson, B., & Yong, D. 2009, ApJ, 704, L66
Meléndez, J., Dodds-Eden, K., & Robles, J. A. 2006, ApJ, 641, L133
Meléndez, J., & Ramírez, I. 2007, ApJ, 669, L89
Meléndez, J., Schuster, W. J., Silva, J. S., et al. 2010, A&A, 522, A98
Menzies, J. W., Cousins, A. W. J., Banfield, R. M., & Laing, J. D. 1989, S. Afr. Astron. Obs. Circ., 13, 1
Mermilliod, J., Mermilliod, M., & Hauck, B. 1997, A&AS, 124, 349
Perryman, M. A. C., Lindegren, L., Kovalevsky, J., et al. 1997, A&A, 323, L49
Ramírez, I., & Meléndez, J. 2005a, ApJ, 626, 446
Ramírez, I., & Meléndez, J. 2005b, ApJ, 626, 465
Ramírez, I., Meléndez, J., & Asplund, M. 2009, A&A, 508, L17
Stebbins, J., & Kron, G. E. 1957, ApJ, 126, 266
Straizys, V., & Valiauga, G. 1994, Balt. Astron., 3, 282
Strömgren, B. 1963, QJRAS, 4, 8
Tüg, H., & Schmidt-Kaler, T. 1982, A&A, 105, 400
van den Bergh, S. 1965, J. R. Astron. Soc. Can., 59, 253
van Dokkum, P. G. 2001, PASP, 113, 1420